LA-UR-12-23590 (Accepted Manuscript)

Qualitative comparison of bremsstrahlung X-rays and 800 MeV protons for tomography of urania fuel pellets

Morris, Christopher; Bourke, Mark A.; Byler, Darrin D.; Chen, Ching-Fong; Hogan, Gary E.; Hunter, James F.; Kwiatkowski, Kris K.; Mariam, Fesseha G.; McClellan, Kenneth J.; Merrill, Frank E.; Morley, Deborah J.; Saunders, Alexander

To be published in: Review of Scientific Instruments

DOI to publisher's version: 10.1063/1.4789947

Permalink to record: http://permalink.lanl.gov/object/view?what=info:lanl-repo/lareport/LA-UR-12-23590

Qualitative Comparison of Bremsstrahlung X-rays and 800 MeV Protons for Tomography of Urania Fuel Pellets

C. L. Morris,[1] M. Bourke, D. D. Byler, C. F. Chen, G. Hogan , J. F. Hunter, K. Kwiatkowski, F. G. Mariam, K. J. Mcclellan, F. Merrill, D. J. Morley, and A Saunders

Los Alamos National Laboratory, Los Alamos , NM 87544

Abstract We present an assessment of x-rays and proton tomography as tools for studying the time dependence of the development of damage in fuel rods. We also show data taken with existing facilities at Los Alamos National Laboratory that support this assessment. Data on surrogate fuel rods has been taken using the 800 MeV proton radiography (pRad) facility at the Los Alamos Neutron Science Center (LANSCE), and with a 450 keV bremsstrahlung X-ray tomography facility. The proton radiography pRad facility at LANSCE can provide good position resolution (<70 μm has been demonstrate, 20 μm seems feasible with minor changes) for tomography on activated fuel rods. Bremsstrahlung x-rays may be able to provide better than 100 μm resolution but further development of sources, collimation and detectors is necessary for x-rays to deal with the background radiation for tomography of activated fuel rods.

I. Introduction

Despite the accident at Fukushima, nuclear energy will remain part of the US energy mix for the foreseeable future. Safety margins and predictions of the engineering performance of nuclear reactor fuel rely on modeling codes. These are used to predict dimensional change, stress state and fission gas release as a function of burn up and temperature history. Since the composition and structural integrity of fuel pellets evolves during their duration in a reactor, the ability to predict from first principles the thermophysical properties of Urania (UO2) holds the key to improved performance codes. One problem in advancing models of nuclear fuel performance lies in the need for experimental data of stoichiometry, crystal structure, density, isotope distribution, microstructure and temperature over length scales from submicron to millimeters, across extreme temperature gradients (e.g <1000K over a few mm), in situ, in the bulk under kinetic conditions and to do all of this with 3D resolution.

A new facility at the Los Alamos Neutron Science Center (LANSCE), the material test stand (MTS), is being proposed as a high intensity neutron source for testing new concepts for reactor fuel rods. The ability to nondestructively monitor neutron induced damage in fuel rods has been proposed as part of this facility with the aim of advancing models and providing validation data for performance codes. Both in-situ and ex-situ radiographic options are under study. In both cases radiography needs to be performed in the presence of intense background radiation. Limited success has been attained in nondestructive assay of nuclear fuel rods using neutron radiograhphy and an indirect method of

[1] Author to whom correspondence should be addressed. Electronic mail: cmorris@lanl.gov.

detecting transmitted neutrons using neutron activation.[1, 2] In this report we compare two options for providing three dimensional images of fuel rods, x-ray and proton tomography.

The goal of these studies is to provide time dependent information on the development of radiation induced damage. The length scale of the damage covers dimensions down to the atomic scale. It is desirable to have the best position resolution that can be obtained for objects at the cm scale. Realistically, existing detectors probably limit the position resolution to ~several×10^{-4}-10^{-3} of the linear field of view needed for the tomography. In the experiments presented below the field of view was ~5 cm, so one might hope to obtain ~5-50 μm of position resolution for these objects. The challenge is to demonstrate resolution at this scale for objects with areal densities of 10 g/cm^2 of uranium oxide or thorium oxide with a technology that is robust enough to be used in a radiation field that can be larger than 200 Gy/hr at 30 cm from the fuel rod.

We compare a 450 keV bremsstrahlung X-ray system[3] and 800 MeV proton radiography[4] for this application. We present results of estimates of signal to noise for an activated fuel rod and show tomographic results from surrogate fuel a set of uranium dioxide samples 0.4 cm in diameter of areal density of about 4 g/cm^2. The urania surrogate fuel rod consisted of sintered urania pellets sealed in a 304 stainless steel tube with stainless steel end plugs and an internal spring to restrict pellet movement. The pellets were fabricated to approximately 90% of theoretical density and contain intentional tungsten inclusions added in order to coarsely represent features of interest in irradiated fuel.

II. X-ray Resolution Dose and background

The dose is a function of the size of the features of interest and the thickness of the sample. Below we calculate the dose needed to observe a 50 μm radius feature in a 1 cm thick sample of uranium oxide at a density of 10 g/cm^3 at the one sigma level. The noise was assumed to be dominated by counting statistics of the transmitted beam. Experimental effects that increase the noise, such as scatter background (which can be important), and energy spread (we have assumed mono energetic x-ray spectra) are not included in this estimate.

In transmission radiography, the transmitted flux through an object is used to measure its areal density. The transmission, $t_\lambda(x,y)$, is given in terms of the path length *l(x,y)* through the object and mean free path λ by Beer's law:[5]

$$t_\lambda(x,y) = e^{-\frac{l(x,y)}{\lambda}}. \qquad 1)$$

This can be inverted to calculate the thickness of the object as:

$$l(x,y) = -\lambda \ln(t_\lambda(x,y)). \qquad 2)$$

Here, λ, is given by:

$$\lambda = \frac{1.}{\rho\sigma}, \qquad 3)$$

where ρ is the material number density and σ is the interaction cross section. The scaled length is replaced by a sum over materials for composite objects. The uncertainty in the length determination can be found by taking the derivative of equation 2) with respect to t_λ, and assuming that the uncertainty of the transmitted flux is given by the Normal distribution of the number of transmitted particles. This gives:

$$\frac{dl(x,y)}{dt_\lambda} = -\lambda \frac{1}{t_\lambda(x,y)},$$

so

$$\frac{\Delta l(x,y)}{l(x,y)} = -\frac{\lambda}{l(x,y)t_\lambda(x,y)}\Delta t_\lambda(x,y) \qquad 4)$$

$$= -\frac{\lambda}{l(x,y)} e^{\frac{l(x,y)}{2\lambda}} \frac{1}{\sqrt{N_0(x,y)}}$$

Here $N_0(x,y)$ is the incident fluence. We have applied eq 4) to calculating the dose needed to observe a 50 μm radius defect at the center of fuel rods with diameters of 4 mm and 10 mm at the 1 sigma level. Particle flux was converted to dose using the simplifying assumption of mono-energetic gamma rays and using: $1\ \mathrm{Gy} = 1.25 \cdot 10^{10} E/\lambda$, where λ is the mean free path and *E* is the gamma energy.[6]

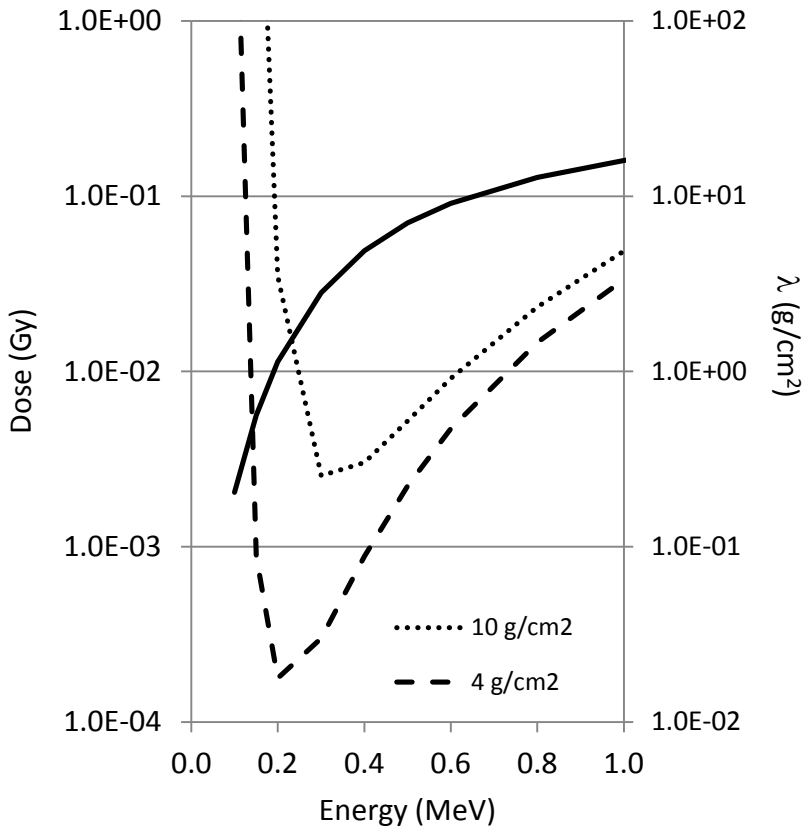

Figure 1) Dose needed to observer a 50 μm radius void at one sigma in a 10 g/cm^2 urania sample (dotted) and a 4 g/cm^2 urania sample (dashed) as a function of x-ray energy (left axis). Solid line) x-ray mean free path, λ, in uranium oxide (right axis).

The CYGNUS x-ray machine [7] at the Nevada test site is a flash radiography machine that provides a sub-millimeter spot, a dose of 0.04 Gy at 1 meter from the source in a 60 ns long pulse. The electron current is 60 kA and the energy is 2.25MeV. Although this is an adequate x-ray source for this application CYGNUS can provide only 2 pulses per day, so it is not suitable for fuel rod tomography. Scaling the CYGNUS parameters suggest that a 2 MV electron source that provides electron pulses of 8 mC would provide doses of 0.01 Gy, 1 meter from the source. The target heat load for a 2 MV, 8 mA source operating continuously would be 16 kW. Water cooling should be able to handle this heat load. The background dose from the fuel rod is expected to be on the order of 0.06 Gy/s at one meter from the target. This dose is the unattenuated dose and is ~ 2 orders of magnitude higher than the transmitted dose for a 1 sec long pulse from a continuous source. X-ray tomography requires a solution to this background problem. Continuous current sources can provide large doses. A microtron source in Los Alamos operating at 6 MeV provides ~0.1 Gy/s at one meter. This could still be overwhelmed by the direct dose from an activated fuel rod.

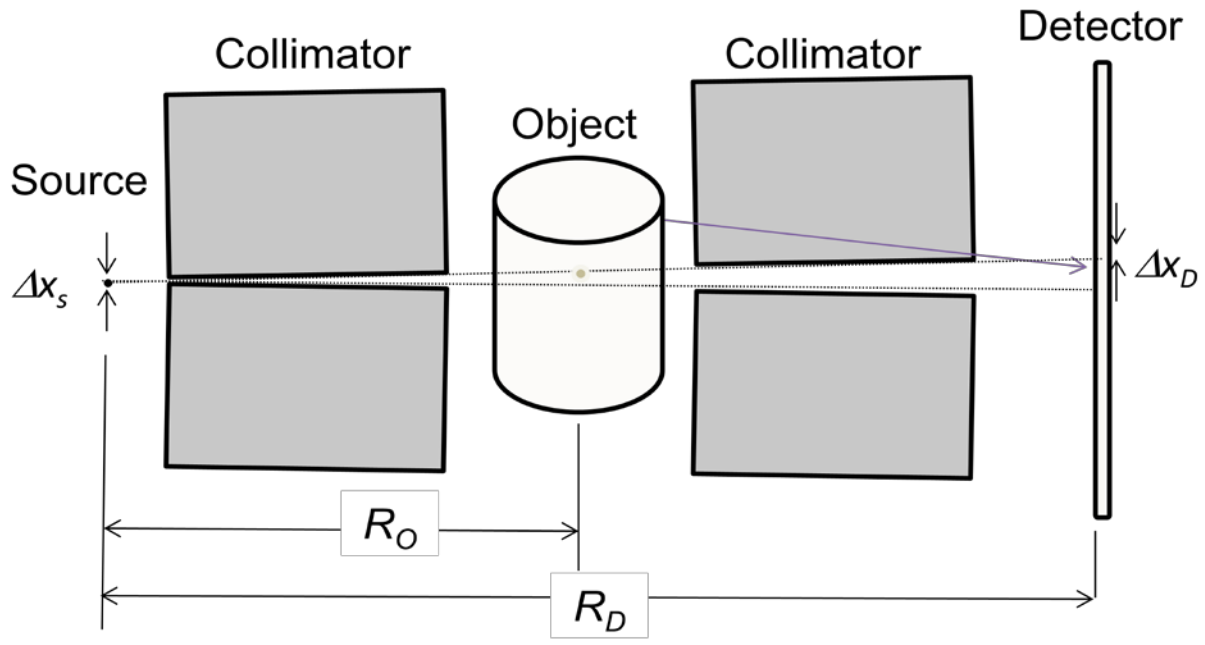

Figure 2) Schematic of an x-ray geometry. The x-ray position resolution is determined by simple geometry to be a function of the source spot size and the detector resolution. A collimator can shield the detector from radiation from the object but also reduces the field of view to narrow slices of the object. Tomographic images may be taken by shifting the object and performing rotations for each slice. Δx_S is the x-ray source size and Δx_D is the detector resolution.

Position resolution is another important issue. At lower energies micro-focus x-ray systems with extraordinarily good position resolution are available. These systems are limited to ~250 keV which is insufficient for the materials under consideration. The spatial resolution at the object location, Δx, can be calculated:

$$\Delta x = \sqrt{\Delta x_S^2 \frac{(R_D - R_O)^2}{R_O^2} + \Delta x_D^2 \frac{R_D^2}{R_O^2}} \quad 5)$$

where Δx_s and Δx_D are the source spot and the detector resolution respectively, R_O is the distance between the source and the object and R_D is the distance between the detector and the object. State of the art source sizes for MV x-ray sources is ~1 mm. Thin detectors can provide very good detector resolution, but have very low efficiency. In thicker detectors the resolution is determined by multiple Coulomb scattering of the energetic electron produced by the gamma ray interaction. The range of a 0.3 Me V electron is 800 μm in CsI. The multiple scattering angle is ~π in a 1 mm thick slab of CsI. Such a detector would have ~ 40% detection efficiency for 300 keV x-rays and optimistically might provide 150 μm position resolution. A new high energy radiography system designed by Lawrence Livermore National Laboratory, CoLLOSIS, utilizing TbO2 scintillator glass and turning mirrors to 4Kx4K CCDs has demonstrated better than 100 micron resolution with 30 micron pixel size using a 9MeV linear accelerator but it has not been designed for high activity objects.

If the detector resolution is less than the source resolution the favored geometry is (RD-RO)<RO. A suitable geometry is $\frac{R_D - R_O}{R_O} = 10$. In this configuration the detector sees the entire background dose from the object, 6 R/sec. It is important to reduce the background dose in order to obtain a suitable signal to noise ratio.

One method for improving the signal to noise is to use collimators, as shown in Figure 2. The dose from the target can be reduced by 2 orders of magnitude with a 10 cm thick heavy metal shield (lead, gold, tungsten or tantalum). The background dose can be reduced at the expense of the exposure time needed for exposing many slices.

The risks in obtaining ~50 μm with bremsstrahlung x-ray systems are source dose rate, source spot size, detector resolution, and most importantly noise introduced by the objects activity. The first three issues have been addressed in other applications but the activity of the fuel rods remains a major obstacle which may affect the solution of the first three.

III. Resolution Dose and Background in Proton Radiography

In proton radiography (pRad) there are two components to the attenuation, $\tau = \tau_\lambda \tau_c$.[8] The first term is due to nuclear absorption and scattering and the second is due to Coulomb multiple scattering. Proton radiography relies on lenses to restore position resolution lost due to the Coulomb multiple scattering. The ratio of images in a two lens proton radiography system separates the loss of flux due to multiple scattering from the nuclear attenuation loss. If the multiple scattering angular distribution is given by a Gaussian, the transmission through an aperture is given by:

$$t_c = (1 - e^{-\frac{\kappa}{l}})$$
$$\text{where:}$$
$$\kappa = \frac{\theta^2 p^2 \beta^2 X_0}{2 \times 14.1^2} \qquad 6)$$

The length scale κ for multiple scattering radiography can be chosen by using an angle collimator to select θ.

An error analysis can be performed by taking the derivative of eq 6) with respect to *l*:

$$\frac{dt_c}{dl} = \frac{\kappa}{l^2} e^{-\frac{\kappa}{l}}. \qquad 7)$$

The relative uncertainty in the measurement of *l* is:

$$\frac{\Delta l}{l} = \frac{l}{\kappa} \frac{\sqrt{t_c}}{1-t_c} \frac{1}{\sqrt{N_0}}, \qquad 8)$$

Where, as in the x-ray case, the uncertainty in the measurement of transmission is assumed to be due to counting statistics. The dose needed to achieve 1% areal density resolution along with the expected position resolution is plotted as a function of collimator angle in Figure 3 for an 800 MeV beam. The collimator, an integral part of pRad, is schematically indicated in Figure 4

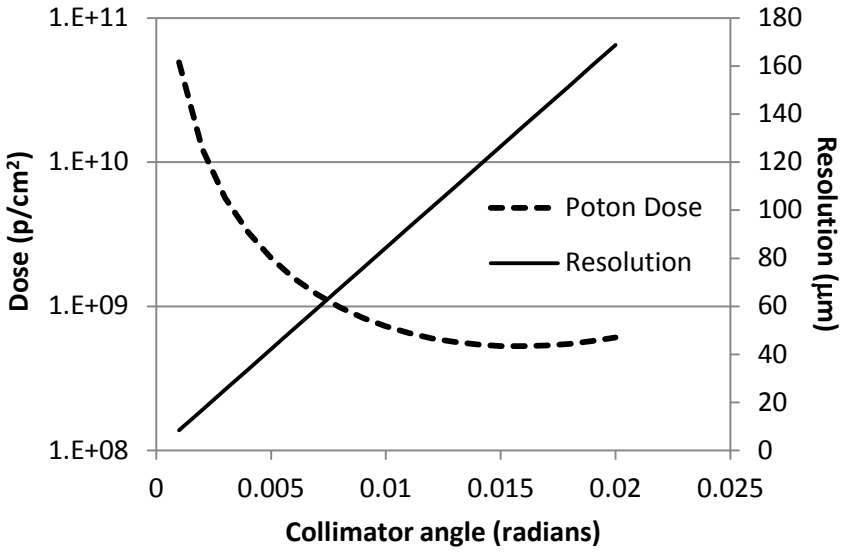

Figure 3) Proton flux required to observe a 50 μm radius void in a 1 cm thick thoria or urania fuel rod (dashed line) and resolution (solid line) as a function of collimator angle.

The position resolution has been calculated assuming that it is dominated by chromatic aberrations from the imaging lens.[9, 10] It is given by: $\Delta x = T_{126}\frac{\Delta p}{p}\Delta\theta$. Here Δx is the position resolution, $\Delta\theta \sim \frac{\theta_{collimator}}{2}$ is the rms of the transmitted angular distribution, $\frac{\Delta p}{p}$ is the momentum spread of the transmitted beam, and T_{126} is the chromatic length of the lens. In Figure 3, a momentum spread given by 1 g/cm^2 of focus spread (10% of the thickness of the thoria fuel rods measured below). This can be achieved using a graded energy degrader-a technique commonly employed in static proton radiography for reducing the energy spread of the transmitted beam. The data we show below were taken with a 7.5 mR collimator.

The background dose transmitted through the lens system can also be estimated. There is a large reduction due to the distance from the object to the detector. There is also a reduction in the background due to the proton collimator in the lens system. If the collimator dimension is small

compared the source, then the dose can be estimated by treating the collimator as a pinhole imager of the object. The dose at the collimator location, $D_{image} = D_{30}\left(\frac{0.3}{R_{collimator}}\right)^2$

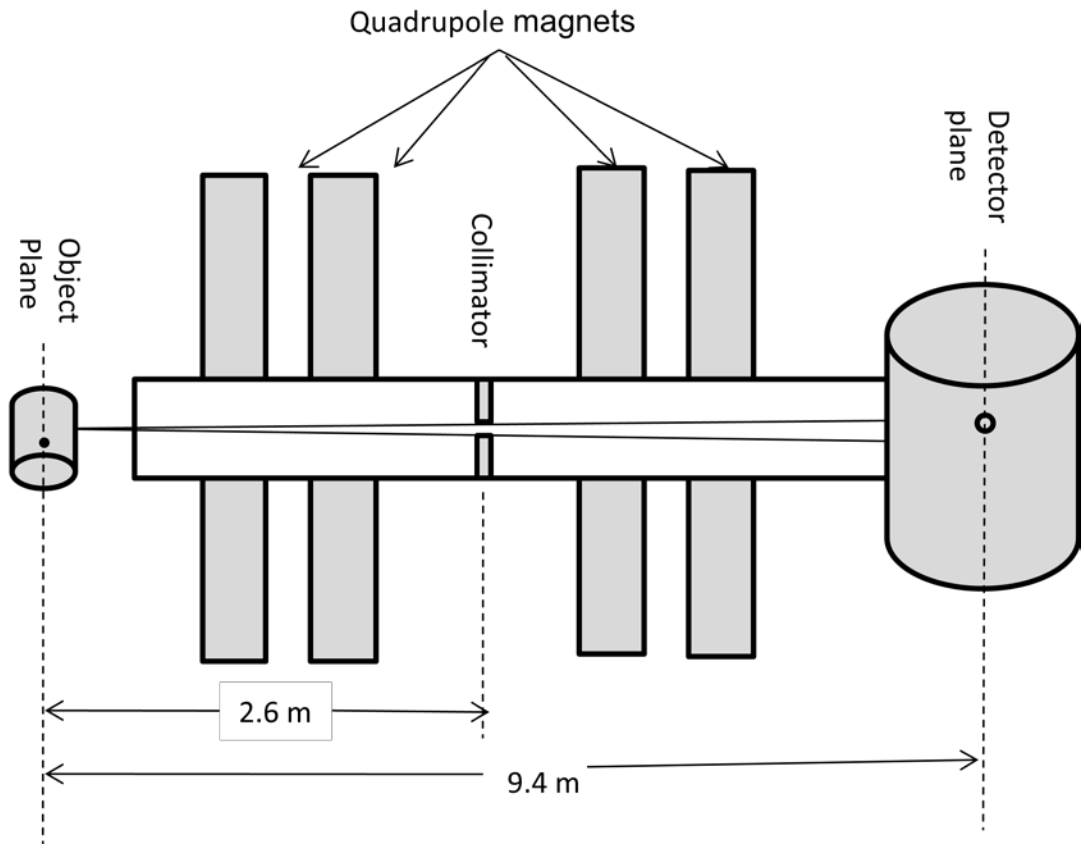

Figure 4) Schematic layout of a proton radiography system.

IV. X-ray and proton tomography comparison

Both the pRad and X-ray studies were pursued as proof of principal tests using existing equipment to explore the viability of tomographic measurements on material used in nuclear fuel pellets with dimensions consistent with fast reactor fuel. Experimental and analytic improvements would improve the resolution of both techniques.

Results from applying the proton radiography tomographic analysis tools to the 450 keV tomography of a UO_2 fuel rod surrogate are presented here. Data were taken in 150 steps covering 360 degrees. A 450 kV Philips x-ray source with a 2mmSn+0.5mmCu filter was used with a custom low scatter Varian Paxscan amorphous silicon detector.[11] The source to object distance was 1.91 m and the source to detector distance as 2.225m. Data were taken in equal angle steps between 0 and 360 degrees. Each

image was constructed from an average of 20 exposures taken at a rate of 0.5 Hz. Angles were advanced a rate of 0.025 Hz

The data, originally taken on 127 μm pixels at the detector were remapped onto 50 μm pixels, using a Monte Carlo sampling technique, and then inverted using filtered back projection. It was necessary to use a filter frequency of 0.25 in order to suppress radial artifacts in the reconstruction.

Areal densities were calculated using Eq 2) and adjusting λ to gave the nominal area density at the center of the fuel pin.

Proton data were taken using a permanent magnet lens system that provides a magnification of about 2.7.[1 12]Proton images in the image plane of the lens were made on a 350 μm thick columnar CsI(Tl) screen, and recoded on a set of 5 three frame CMOS imaging cameras.[8] Seven hundred and twenty frames of data were taken covering 180 degrees. Each frame was formed from an average of 15 camera pictures taken using 3 beam pulses of 6×10^9 protons distributed as a two dimensional Gaussian across the 4×4 cm^2 field of view at the object location with a widths of 1.3 cm (sigma) in each direction. The proton data were taken at a rate of 0.5 Hz. The rate was limited by the speed at which the goniometer could reliably rotate the object.

A photography of the system is shown in Figure 5. Also shown is a schematic drawing of how the fuel pin could be mounted in a shielding cast to provide radiation protection for the experimenters.

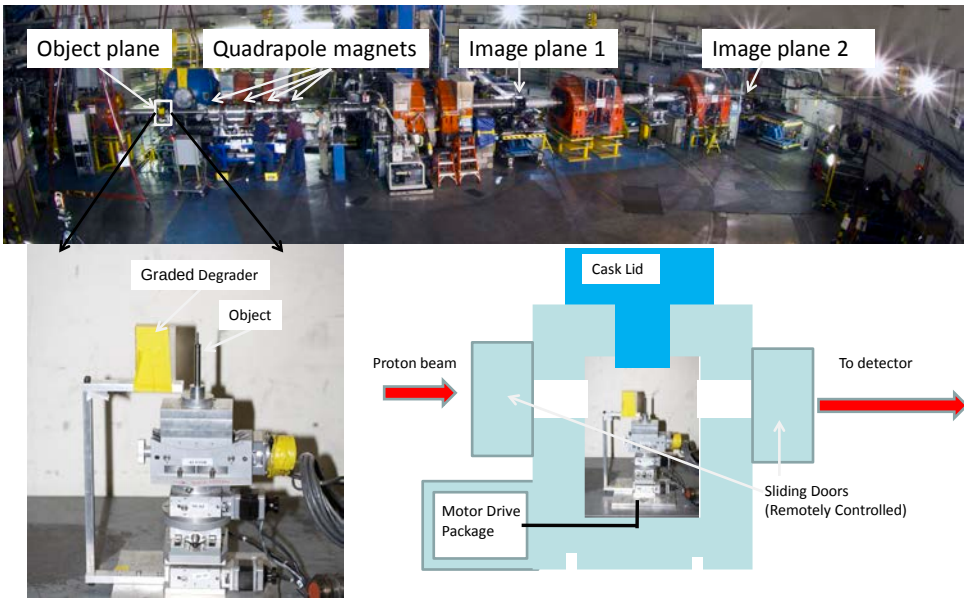

Figure 5) Proton radiography system. Picture at top shows the proton radiography system. Bottom left) the graded degraded, goniometer, and the lead rod object. Bottom right is a schematic representation of how an object could be mounted in a cast to provide radiation shielding.

The proton energy loss across the fuel rod image was flattened using an energy degrader that was mounted directly up stream of the fuel rod (shown in the insert at the lower left in Figure 5). The degrader was built from polyethylene to minimize the ratio of energy loss to multiple scattering and was designed to minimize the spread in transmitted energies across the field of view while not introducing high special frequency artifacts. The data were processed by dividing each image by the beam distribution, dividing by a target out image of the degrader, normalizing the images to unity by dividing by a two dimensional polynomial fit to the data outside of the fuel rod, and by inverting the transmission using Eq. 6) to obtain areal densities. Examples of the results of this processing can be seen in reference [13]. The fuel rods were measured to be a single phase material using X-ray diffraction (XDR), either thoria or urania. The parameters used for the inversion were obtained by fitting transmission through a 1.27 cm diameter lead rod, and appropriately scaled for thoria and urania.

The graded degrader was misaligned with the object. This led to radial artifacts in the reconstruction that were not entirely symmetric because the angular range of the tomographic data only covered 180 degrees. A position dependent correction function was derived by assuming that a median average of radial slices at different positions through a rod could be represented by a constant density. Each slice was divided by the median average and then multiplied by the average density. The geometry for the x-ray tomography was conical, as is typical, because of the point source nature of the x-ray beam. For proton tomography the beam is very nearly parallel,

A comparison of the areal density obtained at one angle from the two radiographies is shown in Figure 5.

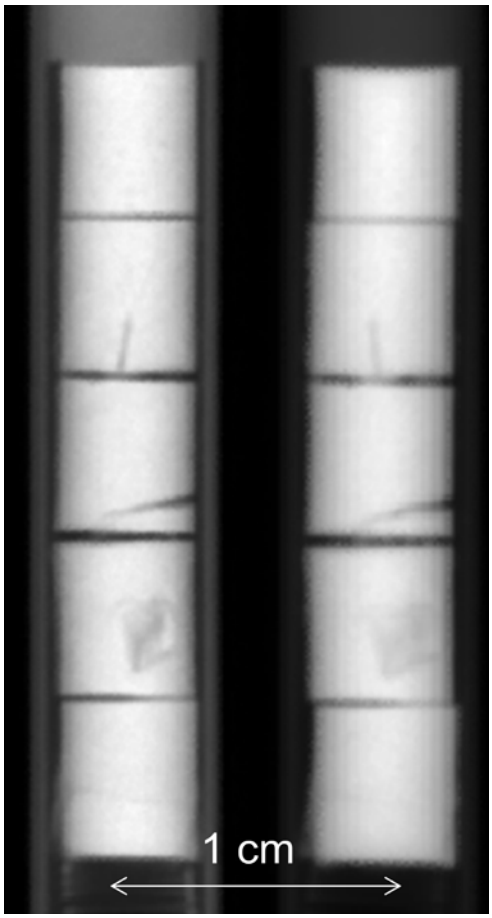

Figure 6) Areal density Left) proton radiography Right) X-ray radiography. The rotation between the feature in the second pellet from the top is an assembly difference between the two experiments.

Volume densities were calculated from both the x-ray and the pRad data using filtered back projection. Care was taken to maintain the correct position and density scaling for both techniques. A lower frequency filter was required to avoid artifacts in the x-ray data since the remapping of pixels violated the Nyquist criteria for data sufficiency in reconstruction. . A Comparison of the pRad and x-ray reconstructions is shown in Figure 6 as slices through the center of the rod. The x-ray reconstructions are not flat because of a significant scatter background as well as beam-hardening affects.

The scatter background was subtracted by transforming the initial data:

$$R'(x,y) = -\lambda\, ln\left(\frac{e^{-\ln(R(x,y)}-b}{1-b}\right). \quad 9)$$

The background, *b,* was adjusted to flatten the reconstruction of the uranium pellets where λ=*1.1* g/cm^2, the effective x-ray mean free path, was adjusted to give the correct path length through the center of the pellets. The transmission through the center of the rod before background correction was 0.053. The background that gave a flat reconstruction was found to be 0.035±.002.

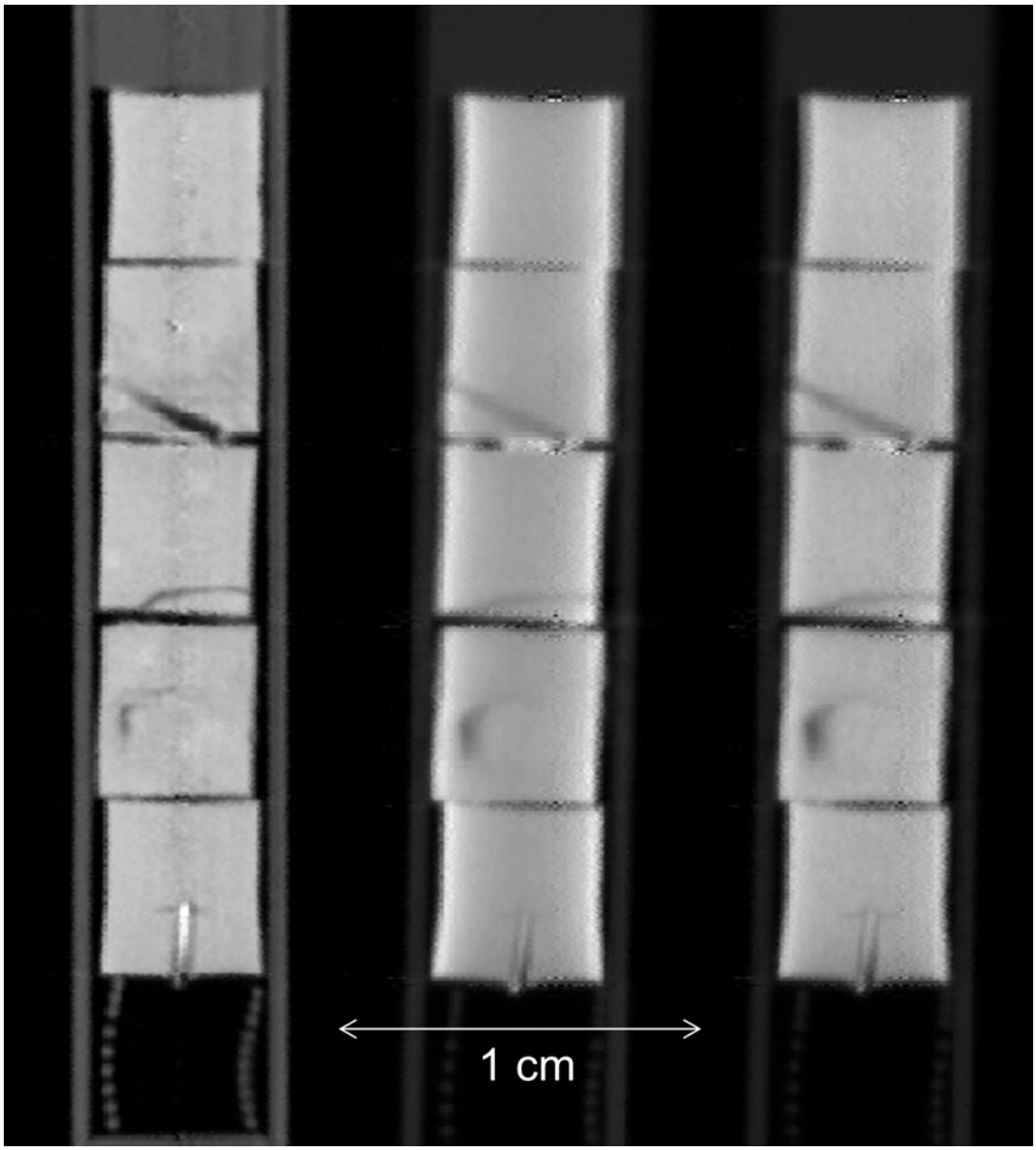

Figure 7) Comparable slices measured with proton (left), x-ray (center), and background corrected x-ray tomography. We note that no background correction is needed for the proton data.

The signal to noise ratio in the lowest transmission part of the radiography was 0.51, suggesting that without background mitigation it will be difficult to radiograph the thicker thorium pins. The effective mean free path was found to be 0.91 g/cm^2.

Plots showing the effect of the background correction on the density reconstruction are shown in Figure 7. Also, the line density plots through one of the defects so the greater detail that can be obtained in proton radiography.

.

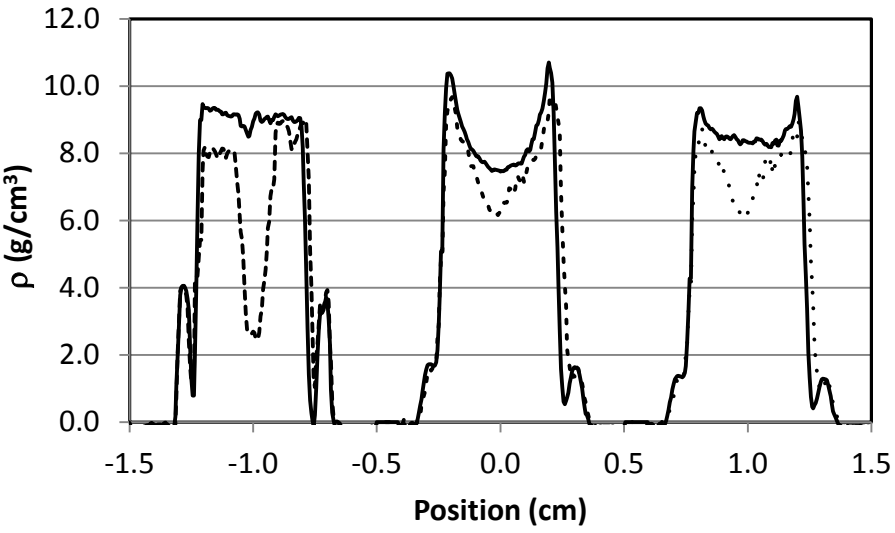

Figure 8) Densities for lineouts along a horizontal line in the center of the center pellet in Figure 6 (solid line) and through the diagonal defect in the fourth pellet from the bottom (dashed line) . Left) proton tomography, center) X-ray tomography with no background correction, right) x-ray tomography with background correction.

The resolution was measured by calculating the function: $E(x,y) = \sqrt{\nabla \cdot \nabla \rho(\mathrm{x},\mathrm{y})}$ where, $\rho(x,y)$ was a slice of reconstructed densities taken from the center of the object and fitting a Gaussian to the result(Figure 9). The position resolution in the proton experiment was measured to be 70 μm, and in the X-ray experiment it was 150 μm.

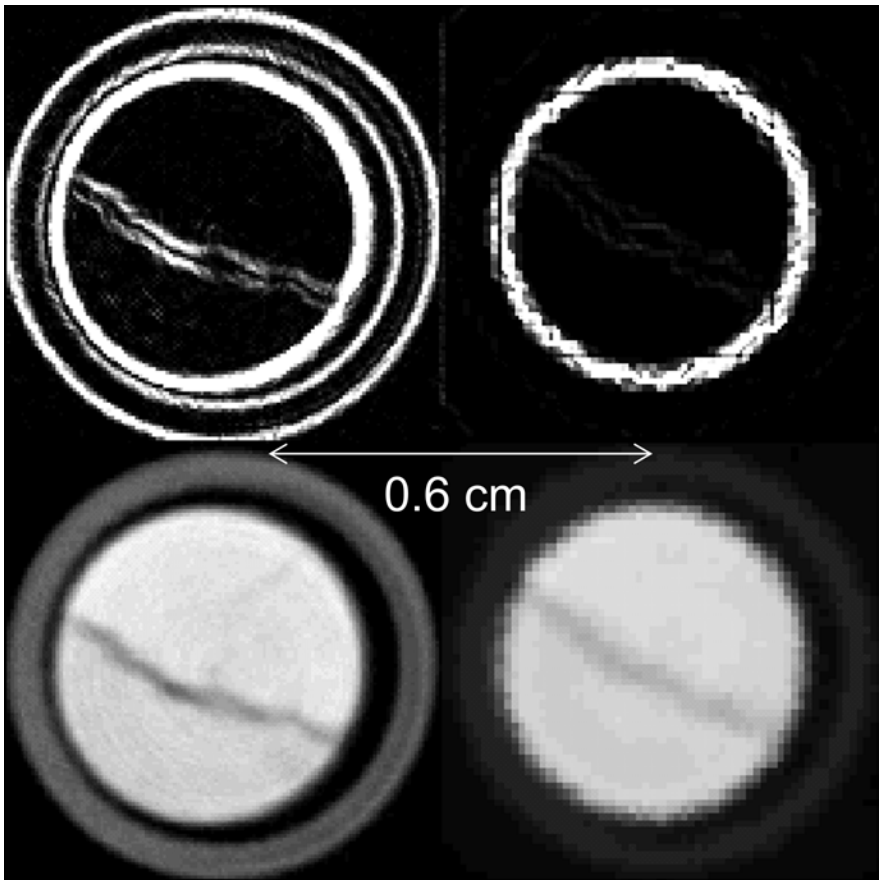

Figure 9) x-y cross section through the center of the reconstructed densities for prad (left) and xrad (right) for one of the unania pellets. The bottom panels show density, the top panels show the edge function. This section is taken through the crack visible in the lower part of the third pellet from the bottom in Figure 7.

V. Thoria Results

Data were also taken on 1 cm diameter thoria test objects mounted in a stainless steel case. Although the x-ray data showed no structure, presumably due to low transmission and scatter background, the proton data were similar in quality to the data on the thinner (0.4 cm) urania samples. A slice through the center of the proton tomographic reconstructed assemble is shown in Figure 9. The resolution and density precision were sufficient to resolve texture and small defects in the samples. This test illustrates the larger dynamic range of proton radiography in thickness when compared with a fixed energy bremsstrahlung x-ray system.

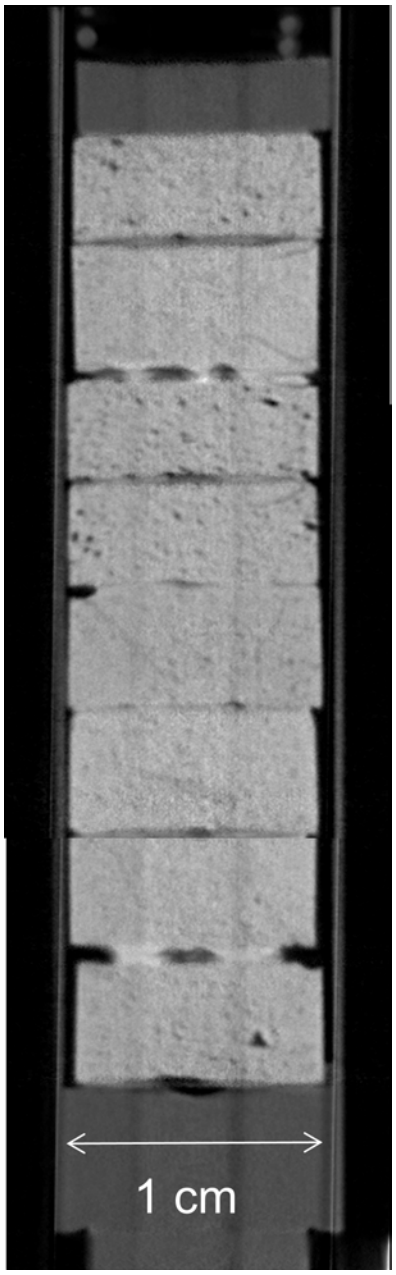

Figure 10) Slice through a tomographic reconstruction of part of the throria test assembly. The two vertical strips extending through the object are reconstruction artifacts.

VI. Conclusion

The experiments showed that both 450 KeV X-rays from a brehmsstrahlung x-ray system and 800 MeV Prad have sufficient intensity and penetration to perform tomography 4 mm diameter urania fuel pellets fabricated as surrogates for nuclear fuel. The spatial resolution of both techniques are primarily limited by detector resolution at this time but spatial resolution of better than 100 microns is clearly achievable

Improvements in x-ray tomography require a higher energy source, small spot size, better collimation, and higher resolution detectors. All of these improvements have been achieved with existing systems but their successful application to a high activity object is uncertain. Proton radiography data can be improved with higher incident energy, improved optics, tighter collimation, and higher resolution detectors. The only additional capability to enable tomography of activated fuel rods using the 800 MeV proton radiography facility at LANSCE is remote sample handling so that biological exposures can be limited to those external to a shielding cast.

1. F. Groeschel, P. Schleuniger, A. Hermann, E. Lehmann, et al., Nuclear Instruments and Methods in Physics Research Section A: Accelerators, Spectrometers, Detectors and Associated Equipment **424** (1), 215-220 (1999).
2. M. Tamaki, K. Iida, N. Mori, E. H. Lehmann, et al., Nuclear Instruments and Methods in Physics Research Section A: Accelerators, Spectrometers, Detectors and Associated Equipment **542** (1), 320-323 (2005).
3. W. C. Roentgen, Nature (UK) **53**, 274 (1896).
4. C. Morris, J. W. Hopson and P. Goldstone, Los Alamos Science **30** (2006).
5. A. Beer, Ann. Phys. Chem. **86**, 78-90 (1852).
6. K. Nakamura, K. Hagiwara, K. Hikasa, H. Murayama, et al., Journal of Physics G: Nuclear and Particle Physics **37** (7A), 075021 (2010).
7. T. H. Braid, D. S. Gemmell, R. E. Holland, W. J. Pietsch, et al., Phys Rev B **19** (1), 130-134 (1979).
8. K. Kwiatkowski, P. Nedrow, V. Douence, F. Mariam, et al., Nuclear Instruments and Methods in Physics Research Section A: Accelerators, Spectrometers, Detectors and Associated Equipment (2010).
9. G. Bucky, American Journal of Roentgenology and Radium Therapy **42**, 428-435 (1939).
10. G. B. Bush, British Journal of Radiology **11**, 611-622 (1938).
11. T. Mottershead, D. Barlow, B. Blind, G. Hogan, et al., 2003 (unpublished).
12. F. Merrill, E. Campos, C. Espinoza, G. Hogan, et al., Review of Scientific Instruments **82**, 103709 (2011).
13. C. Morris, E. Ables, K. Alrick, M. Aufderheide, et al., J. Appl. Phys. (USA) **109**, 104905 (2011).